Thermal Science and Engineering Progress 1 (2017) 39–52

Contents lists available at ScienceDirect

Thermal Science and Engineering Progress

journal homepage: www.elsevier.com/locate/tsep

Thermal performance analysis of a natural convection porous fin with temperature-dependent thermal conductivity and internal heat generation

M.G. Sobamowo [a,*], O.M. Kamiyo [a], O.A. Adeleye [b]

[a] Department of Mechanical Engineering, University of Lagos, Akoka, Lagos, Nigeria
[b] Department of System Engineering, University of Lagos, Akoka, Lagos, Nigeria

ARTICLE INFO

Article history:
Received 29 December 2016
Received in revised form 17 February 2017
Accepted 25 February 2017

Keywords:
Galerkin's method of weighted residual
Natural convection
Porous fin
Thermal performance
Temperature-dependent thermal conductivity and internal heat generation

ABSTRACT

In this study, thermal performance analysis of a natural convection porous fin with temperature-dependent thermal conductivity and internal heat generation is carried out using Galerkin's method of weighted residual. The developed symbolic heat transfer models are used to investigate the effects of various parameters on the thermal performance of the porous fin. It is found that increase in porosity parameter, Nusselt, Darcy and Rayleigh numbers and the thickness-length ratio of the fin increase the rate of heat transfer from the base of the fin and consequently improve the efficiency of the fin. Also, decreasing thermal conductivity parameter results in an increase in the rate of heat transfer from the base of the fin. However, an optimum value is reached beyond which further increase in porosity, Nusselt, Darcy and Rayleigh numbers, thermal conductivity ratio and thickness-length ratio has no significant influence on the rate of heat transfer. For the purpose of verification of the results, exact analytical solutions are developed. The results of the Galerkin's method for the second-order approximation function are found to be in excellent agreements with the results of the exact analytical solutions and also with that of the numerical methods and homotopy perturbation method.

1. Introduction

Heat transfer enhancement in extended surfaces has been a subject of vital importance which has led to extensive research on the use of porous fins. The pioneer work on the heat transfer enhancement through the use of porous was carried out by Kiwan and Al-Nimr [1]. They applied numerical method to investigate the thermal analysis of porous fin while Kiwan [2–4] developed a simple method to study the performance of porous fins in natural convection environment. Also, the same author investigated the effects of radiative losses on the heat transfer from porous fins. Gorla and Bakier [5] numerically carried out the thermal analysis of natural convection and radiation in a rectangular porous fin. Kundu and Bhanja [6] presented analytical model for the analysis of performance and optimization of porous fins. Kundu et al. [7] proposed a model for computing maximum heat transfer in porous fins. Taklifi et al. [8] investigated the effects of magnetohydrodynamics (MHD) on the performance of a rectangular porous fin. In the work, the authors stated that by imposing MHD in system except near the fin tip, heat transfer rate from the porous fin decreases. Bhanja and Kundu [9] analytically investigated thermal analysis of a constructal T-shape porous fin with radiation effects. An increase in heat transfer is found by choosing porous medium condition in the fin. Recently, Kundu et al. [10] studied the performance and optimum design analysis of porous fin of various profiles operating in convection environment transient heat transfer analysis of variable section pin fins. Saedodin and Sadeghi [11] analyzed the heat transfer in a cylindrical porous fin while Saedodin and Olank [12] analyzed temperature distribution in porous fin in a natural convection condition. Darvishi et al. [13] studied the thermal performance of a porous radial fin with natural convection and radiative heat losses while Hatami and Ganji [14] investigated the thermal performance of circular convective-radiative porous fins with different section shapes and materials. Hatami et al. [15–18] presented various heat transfer studies in both dry and wet porous fins. All the previously cited studies on porous fin are based on constant thermal conductivity. Such assumption might be correct because, for ordinary fins problem, the thermal conductivity of the fin might be taken to be constant.

* Corresponding author.
E-mail address: mikegbeminiyiprof@yahoo.com (M.G. Sobamowo).

http://dx.doi.org/10.1016/j.tsep.2017.02.007
2451-9049/

Nomenclature

a_r	aspect ratio of the porous fin base area to the surface area
A	cross sectional area of the fins, m^2
A_b	porous fin base area
A_s	porous fin surface area
Bi	Biot number
h	heat transfer coefficient, $W\,m^{-2}\,k^{-1}$
h_b	heat transfer coefficient at the base of the fin, $W\,m^{-2}\,k^{-1}$
c_p	specific heat of the fluid passing through porous fin (J/kg-K)
Da	Darcy number
g	gravity constant (m/s^2)
h	heat transfer coefficient over the fin surface (W/m^2 K)
H	dimensionless heat transfer coefficient at the base of the fin, $W\,m^{-2}\,k^{-1}$
k	thermal conductivity of the fin material, $W\,m^{-1}\,k^{-1}$
k_b	thermal conductivity of the fin material at the base of the fin, $W\,m^{-1}\,k^{-1}$
k_{eff}	effective thermal conductivity ratio
K	permeability of the porous fin (m^2)
L	Length of the fin, m
m	mass flow rate of fluid passing through porous fin (kg/s)
Nu	Nusselt number
P	perimeter of the fin (m)
Q	dimensionless heat transfer rate per unit area
q_b	heat transfer rate per unit area at the base (W/m^2)
Q_b	dimensionless heat transfer rate the base in porous fin
Q_s	dimensionless heat transfer rate the base in solid fin
Ra	Rayleigh number
S_h	Porosity parameter
t	thickness of the fin
T_b	base temperature (K)
T	fin temperature (K)
T_a	ambient temperature, K
T_b	Temperature at the base of the fin, K
v	average velocity of fluid passing through porous fin (m/s)
x	axial length measured from fin tip (m)
X	dimensionless length of the fin
w	width of the fin
q	internal heat generation in W/m^3

Greek symbols

β	thermal conductivity parameter or non-linear parameter
δ	thickness of the fin, m
δ_b	fin thickness at its base
γ	dimensionless internal heat generation parameter
θ	dimensionless temperature
θ_b	dimensionless temperature at the base of the fin
η	efficiency of the fin
ε	effectiveness of the fin
β'	coefficient of thermal expansion (K^{-1})
ε	porosity or void ratio
υ	kinematic viscosity (m^2/s)
ρ	density of the fluid (kg/m^3)

Subscripts

S	solid properties
F	fluid properties
eff	effective porous properties

However, if large temperature difference exists within the fin, typically, between tip and the base of the fin, the thermal conductivity is not constant but temperature-dependent. Also, in their work on porous fins, Gorla et al. [19] and Moradi et al. [20] pointed out that for most materials, the effective thermal conductivity increases with temperature. Such consideration provides a better picture of thermal behaviour or performance of the porous fin. Therefore, while analyzing the fin, effects of the temperature-dependent thermal conductivity must be taken into consideration. In carrying out such analysis, the thermal conductivity may be modelled for such and other many engineering applications by linear dependency on temperature. Such dependency of thermal conductivity on temperature renders the problem highly non-linear and difficult to solve exactly. It is also very realistic to consider the temperature-dependent internal heat generation in the fin (electric-current carrying conductor, nuclear rods or any other heat generating components of thermal systems). In solving the heat transfer problem in porous fin, Kundu [6–7,10] applied Adomian decomposition method (ADM) on the performance and optimum design analysis of the fins while Saedodin and Sadeghi [11], Kiwan [1–5] applied Runge-Kutta for the thermal analysis in porous fin. Golar and Baker [5] and Gorla et al. [19] applied Spectral collocation method (SCM) to study the effects of variable thermal conductivity on the natural convection and radiation in porous fin. Saedodin and Shahababaei [21] adopted homotopy perturbation method (HPM) to analyse heat transfer in longitudinal porous fins while Darvishi et al. [13] and Moradi et al. [20] and Ha et al. [22] adopted homotopy analysis method (HAM)to provide solution to the natural convection and radiation in a porous and porous moving fins while Hoshyar et al. [23] used homotopy perturbation method and collocation method for thermal performance analysis of porous fins with temperature-dependent heat generation. Hatami and Ganji [14] applied least square method (LSM) to study the thermal behaviour of convective-radiative in porous fin with different sections and ceramic materials. Also, Rostamiyaan et al. [24] applied variational iterative method (VIM) to provide analytical solution for heat transfer in porous fin. Ghasemi et al. [25] used differential transformation method (DTM) for heat transfer analysis in porous and solid fin. The approximate analytical methods as applied by past researchers solve the differential equations without linearization, discretization or no approximation, linearization restrictive assumptions or perturbation, complexity of expansion of derivatives and computation of derivatives symbolically. However, the search for a particular value that will satisfy second the boundary condition or the determination of auxiliary parameters necessitated the use of software and such could result in additional computational cost in the generation of solution to the problem. Also, most of the approximate methods give accurate predictions only when the nonlinearities are weak or for small values of the fin thermo-geometric parameter, they fail to predict accurate solutions for strong nonlinear models. Also, the methods often involved complex mathematical analysis leading to analytic expression involving a large number of terms and when they are routinely implemented, they can sometimes lead to erroneous results [26,27]. Moreover, in practice, approximate analytical solutions with large number of terms are not convenient for use by designers and engineers. Inevitably, simple yet accurate expressions are required to determine the fin temperature distribution, efficiency, effectiveness and the optimum parameter. Also, variational methods such as Ritz and Rayleigh-Ritz methods sometimes provide powerful results, such as upper and lower bounds on quantities of interest but require more mathematical manipulations than

method of weighted residual and they are not applicable to all problems, thus they suffer a lack of generality. Conversely, the method of weighted residuals (MWR) can be used to obtain answers of any desired accuracy. In many test cases, MWR compares favorably to finite difference computations in that the MWR results are either more accurate or require less computation time to generate or both. The methods of weighted residual such as collocation method, sub-domain method, Galerkin method and least squares method are easy to apply. Among these methods, the Galerkin method is the most preferable because of its equivalence to the variational method, which gives more accurate values of an eigenvalue. However, in most cases, the criterion can be chosen based on convenience. Also, Lewis et al. [28] submitted that the Galerkin method is the most accurate of the methods of weighted residual. The Galerkin method of weighted residuals provides a very powerful, novel and accurate approximate analytical solution procedure that is applicable to a wide variety of linear and nonlinear problems and thus makes it unnecessary to search for variational formulations in order to apply the finite element method for the problems [29]. In other to reduce the computation cost and task in the analysis of such problem. It solves the nonlinear equation directly without simplification, linearization, perturbation, Taylor's series expansion, mesh independent study and determination of auxiliary parameters and functions as carried out in HPM, HAM, ADM, NM, VIM, and DTM [30]. It reaches final results faster than numerical procedures. Hence, in this work, Galerkin's method of weighted residual is applied for the analysis the thermal performance in porous fin with temperature-dependent thermal conductivity and internal heat generation. The results obtained by the method (for solving the problem under investigation) are compared with the previous studies and excellent agreements are established.

2. Problem formulation

Consider a straight porous fin of length L and thickness t exposed on both faces to a convective environment at temperature T_∞ as shown in Fig. 1.The dimension x pertains to the height coordinate which has its origin at the fin tip and has a positive orientation from fin tip to fin base. In order to analyze the problem, the following assumptions are made.

1. Porous medium is homogeneous, isotropic and saturated with a single phase fluid
2. Physical properties of solid, as well as fluid are considered as constant except density variation of liquid, which may affect the buoyancy term where Boussinesq approximation is employed.
3. Fluid and porous mediums are locally in thermodynamic equilibrium in the domain.
4. Surface convection, radiative transfers, and non-Darcian effects are negligible and only natural convection is considered. Heat is transferred away from the fin base only through the pores i.e. no convective heat transfer to the surrounding.
5. The temperature variation inside the fin is one-dimensional i.e. temperature varies along the length only and remain constant with time.
6. There is no thermal contact resistance at the fin base and the fin tip is an adiabatic type.

Based on Darcy's model and following the above assumptions, the thermal energy balance could be expressed

$$q_x - \left(q_x + \frac{\delta q}{\delta x}dx\right) = \rho c_p v(x) w(T - T_c)dx + q_{\text{int.}}(T)A_{cr}dx \tag{1}$$

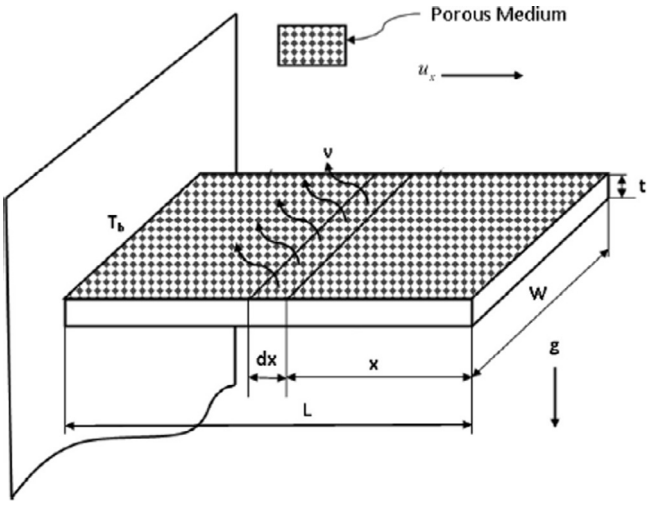

Fig. 1. Schematic of the longitudinal porous fin geometry with the internal heat generation.

The velocity of the buoyancy driven flow v(x) at any location x in the fin is obtained by applying the Darcy's law:

$$v(x) = \frac{g\beta' K}{\upsilon_f}(T - T_\infty) \tag{2}$$

$$q_x - \left(q_x + \frac{\delta q}{\delta x}dx\right) = \frac{\rho c_p g\beta' K}{\upsilon_f} w(T - T_\infty)^2 dx + q_{\text{int.}}(T)A_{cr}dx \tag{3}$$

As $dx \to 0$, Eq. (3) reduces to Eq. (4)

$$-\frac{dq}{dx} = \frac{\rho c_p g\beta' K}{\upsilon_f} w(T - T_\infty)^2 + q_{int.}(T)A_{cr} \tag{4}$$

From Fourier's law of heat conduction

$$q = -k(T)A_{cr}\frac{dT}{dx} \tag{5}$$

Substituting Eq. (5) into Eq. (4), we have

$$\frac{d}{dx}\left(k(T)A_{cr}\frac{dT}{dx}\right) = \frac{\rho c_p g\beta' Kw}{\upsilon_f}(T - T_\infty)^2 + q_{in}(T)A_{cr} \tag{6}$$

Further simplification of Eq. (7) gives the governing differential equation for the fin as given by

$$\frac{d}{dx}\left[k_{eff}(T)\frac{dT}{dx}\right] - \frac{\rho c_p g\beta' K(T - T_\infty)^2}{t\upsilon_f} + q_a(T) = 0 \tag{7}$$

The boundary conditions are

$$\begin{aligned} x &= L, \quad T = T_b \\ x &= 0, \quad \tfrac{dT}{dx} = 0 \end{aligned} \tag{8}$$

For many engineering applications, the thermal conductivity and the coefficient of heat transfer are temperature-dependent. Therefore, the temperature-dependent thermal conductivity and internal heat generation are given by

$$k_{eff}(T) = \phi k_f + (1 - \phi)k_s = k_{eff,a}[1 + \lambda(T - T_\infty)] \tag{9}$$

$$q_{\text{int}}(T) = q_a[1 + \psi(T - T_\infty)] \tag{10}$$

Substituting Eqs. (9) and (10) into Eq. (1), we have

$$\frac{d}{dx}\left[[1 + \lambda(T - T_\infty)]\frac{dT}{dx}\right] - \frac{\rho c_p g K\beta'(T - T_\infty)^2}{k_{eff,a}t\upsilon_f} + \frac{q_a}{k_{eff,a}}[1 + \psi(T - T_\infty)] = 0 \tag{11}$$

On introducing the following dimensionless parameters in Eq. (12) into Eq. (11);

$$X=\frac{x}{L},\quad \theta=\frac{T-T_\infty}{T_b-T_\infty},\quad Ra=Gr.\Pr=\left(\frac{\beta' gT_b t^3}{v_f^2}\right)\left(\frac{\rho c_p v_f}{k_{eff,a}}\right),$$
$$Da=\frac{K}{t^2},\quad Q=\frac{q v_f t}{\rho c_p \beta' gK(T_b-T_\infty)^2}$$
$$S_h=\left(\frac{\beta' g(T_b-T_\infty)t^3}{v_f^2}\right)\left(\frac{\rho c_p v_f K}{k_{eff,a}t^2}\right)\frac{(L/t)^2}{k_{eff,a}}=\frac{RaDa(L/t)^2}{k_{eff,a}},$$
$$\gamma=\psi(T_b-T_\infty),\quad \beta=\lambda(T_b-T_\infty) \tag{12}$$

We arrived at the dimensionless governing differential Eq. (13) and the boundary conditions

$$\frac{d}{dX}\left[(1+\beta\theta)\frac{d\theta}{dX}\right]-S_H\theta^2+S_HQ(1+\gamma\theta)=0 \tag{13}$$

If we expand Eq. (13), the dimensionless governing differential equation become;

$$\frac{d^2\theta}{dX^2}+\beta\theta\frac{d^2\theta}{dX^2}+\beta\left(\frac{d\theta}{dX}\right)^2-S_H\theta^2+S_HQ\gamma\theta+S_HQ=0 \tag{14}$$

The boundary conditions are

$$\begin{aligned} &X=1,\quad \theta=1\\ &X=0,\quad \tfrac{d\theta}{dX}=0 \end{aligned} \tag{15}$$

3. Solution procedure

It is very difficult to develop an explicit exact analytical/closed-form solution for the above non-linear Eq. (14). Therefore, recourse has to be made to either approximation analytical method, semi-numerical method or numerical method of solution. In this work, a simple but very powerful approximate method of solution, Galerkin's method of weighted residual is used.

The Galerkin method of weighted residual is based on the integral of the residual over the domain of interest. In the method, the residual $R(x)$ is weighted over the domain of interest by multiplying $R(x)$ by weighting functions $w_i(x)$ (j = 1, 2 ….), integrating the weighted residuals over the range of integration, and setting the integrals of the weighted residuals equal to zero to give equations for the evaluation of the coefficients C_i of the trial functions $y_i(x)$. Galerkin showed that basing the weighting functions $w_i(x)$ on the trial functions $y_i(x)$ of the approximate solution $y(x)$ yields exceptionally good results. When the governing differential equation is known, it is logical to apply the Galerkin weighted residual approach rather than look for the functional corresponding to the differential equation as in the case of Rayleigh-Ritz.

The procedure of the method is described as follows:

Representing the governing equations by

$$L(\theta)=0\quad in\quad \Omega \tag{16}$$

and

$$\theta\approx\theta^-=\sum_{i=1}^{N}a_iN_i(X) \tag{17}$$

Substitution of the above Eq. (17) into Eq. (16) results in

$$\begin{aligned} L(\theta^-)\quad &\neq 0\\ &=R\ (residual) \end{aligned} \tag{18}$$

The method of weighted residual requires that the parameters $a_1, a_2 \ldots a_n$ be determined by satisfying

$$\int_\Omega w_i(x)Rdx \text{ with } i=1,2,\cdots,n \tag{19}$$

where the functions $w_i(x)$ are the n arbitrary weighting functions. There are an infinite number of choices for $w_i(x)$ but four particular functions are most often used. Depending on the weight function adopted, the method of weighted residual could be collocation, sub-domain, Galerkin or least Square method depending on the choice of the weighting functions. Among all these methods, the Galerkin method is the most accurate method [28]. In the Galerkin's method of weighted residual, the weight function is the same as the trial function. Galerkin's method could be described as a modification of the least squares method. Instead of using the derivative of the residual with respect to the unknown, c_i as done in Least Squares Method, the derivative of the approximating function or trial function is used. In the Galerkin's method of weighted residual, the weight function is the same as the trial function. Since a simple but highly accurate solution is sought, a quadratic trial solution shown in Eq. (20) is adopted in this work. Although, the use of higher degree trial function will produce more accurate results, Ganji [30] pointed out that GM with second degree's trial function converges to result with a good accuracy. Also, Bert [31], having used second degree's trial function in his weighted residual analysis of steady state heat conduction problem and established its high accuracy, pointed out that further refinement is not necessary and therefore, additional terms should not be needed in most instances. Therefore, a second-order approximation function was considered in this work. Given the trial function as

$$\theta=\alpha_1+\alpha_2X+\alpha_3X^2 \tag{20}$$

Eq. (20) satisfies the boundary conditions in Eq. (16) when $\alpha_1=1-\alpha_3,\quad \alpha_2=0$. Thus, the trial function that satisfies the boundary conditions could be written as

$$\theta=1-(1-X^2)\alpha_3 \tag{21}$$

And the weight function is

$$N_i(X)=1-X^2 \tag{22}$$

The Galerkin formulation of the fin equation is

$$\int_0^1 N_i(X)\left[\frac{d^2\theta}{dX^2}+\beta\theta\frac{d\theta}{dX}+\beta\left(\frac{d\theta}{dX}\right)^2-S_H\theta^2+S_HQ\gamma\theta+S_HQ\right]dX \tag{23}$$

Substituting the weight function in Eq. (22) into Eq. (23), we have;

$$\int_0^1 (1-X^2)\left[\frac{d^2\theta}{dX^2}+\beta\theta\frac{d\theta}{dX}+\beta\left(\frac{d\theta}{dX}\right)^2-S_H\theta^2+S_HQ\gamma\theta+S_HQ\right]dX \tag{24}$$

On putting the corresponding terms from Eq. (21) into Eq. (24), it was found that

$$\alpha_3=\frac{7[5(1+\beta)+2S_H(2-\gamma Q)]-7\{[[5(1+\beta)+2S_H(2-\gamma Q)]]^2-[20S_H[\beta+((6/7)S_H)][1-Q(1+\gamma)]]^{\frac{1}{2}}\}}{4[7\beta+6S_H]} \tag{25}$$

If the thermal conductivity of the fin is constant and there is no internal heat generation, then

$$\alpha_3 = \frac{[(7/3) + (35/12S_h)] - \{[(7/3) + (35/12S_h)]^2 - (35/6)\}^{1/2}}{2}$$

Also, substitute Eq. (25) into Eq. (21), we have

$$\theta(X) = 1 - \left\{\frac{5(1+\beta) + 2S_H(2-\gamma Q) - \{[5(1+\beta) + 2S_H(2-\gamma Q)]^2 - [20S_H[\beta + ((6/7)S_H)][1 - Q(1+\gamma)]]\}^{\frac{1}{2}}}{4[\beta + (6/7)S_H]}\right\}(1 - X^2) \tag{26}$$

If the thermal conductivity of the fin is constant and there is no internal heat generation as carried out by Kiwan [3], then by the method in this paper, we arrived at

$$\theta(X) = 1 - \left\{\frac{[(7/3) + (35/12S_h)] - \{[(7/3) + (35/12S_h)]^2 - (35/6)\}^{1/2}}{2}\right\}(1 - X^2) \tag{27}$$

3.1. Heat flux of the fin and rate of heat transfer per unit area from the porous fin

The fin base heat flux is given by Eq. (27)

$$q_b = A_c k(T)\frac{dT}{dx} \tag{28}$$

The dimensionless heat transfer rate at the base of the fin is given by

$$Q_b = \frac{qL}{k_a A_c(T_b - T_\infty)} = \left[(1 + \beta\theta)\frac{d\theta}{dX}\right]_{X=1} \tag{29}$$

Substituting the respective value from Eq. (26) into Eq. (29), we have

$$Q_b = \frac{(1+\beta)\{5(1+\beta) + 2S_H(2-\gamma Q) - [[5(1+\beta) + 2S_H(2-\gamma Q)]] - [20S_H[\beta + ((6/7)S_H)][1 - Q(1+\gamma)]]^{\frac{1}{2}}\}}{2[\beta + (6/7)S_H]} \tag{30}$$

The rate of heat transfer per unit width removed by a porous fin may be calculated from

$$Q_{b/w} = k_a(T_b - T_\infty)\left(\frac{t}{L}\right)\left[(1 + \beta\theta)\frac{d\theta}{dX}\right]_{X=1} \tag{31}$$

Substituting the respective expressions from Eq. (26), the rate of heat transfer from the fin base per unit width is given as

$$Q_{b/w} = k_a(T_b - T_\infty)\left(\frac{t}{L}\right)\frac{(1+\beta)\left\{5(1+\beta) + 2S_H(2-\gamma Q) - [[5(1+\beta) + 2S_H(2-\gamma Q)]] - [20S_H[\beta + ((6/7)S_H)][1 - Q(1+\gamma)]]^{\frac{1}{2}}\right\}}{2[\beta + (6/7)S_H]} \tag{32}$$

3.2. Analysis of heat transfer augmented in porous fin

In order to make a comparison between the heat transfer from a porous fin with that from a solid fin, the ratio of heat transfer rate between the two fins are given by

$$\frac{q_b}{q_s} = \frac{k_{eff}(T)A_b\left(\frac{dT}{dx}\right)_{x=o}}{hA_s(T_b - T_\infty)} \tag{33}$$

where, the denominator represents the maximum possible heat transfer rate obtained using a solid fin. Writing the above equation in terms of the dimensionless temperature, dimension parameters and axial distance, yields

$$\frac{q_b}{q_s} = \frac{A_r}{Nu}\left[(1 + \beta\theta)\frac{d\theta}{dX}\right]_{X=1} \tag{34}$$

Substituting the respective expressions from Eq. (26), we have

$$\frac{q_b}{q_s} = \frac{A_r}{Nu}\left\{\frac{(1+\beta)\{5(1+\beta) + 2S_H(2-\gamma Q) - [[5(1+\beta) + 2S_H(2-\gamma Q)]] - [20S_H[\beta + ((6/7)S_H)][1 - Q(1+\gamma)]]^{\frac{1}{2}}\}}{2[\beta + (6/7)S_H]}\right\} \tag{35}$$

where the area ratio, $A_r = \frac{A_b}{A_s}$

3.2.1. Exact analytical solution for model verification

In order to verify the model results, we developed exact analytical solution for a porous fin with constant thermal conductivity. The dimensionless governing differential equation is given as

$$\frac{d^2\theta}{dX^2} - S_h\theta^2 + S_h Q\gamma\theta + S_h Q = 0 \tag{36}$$

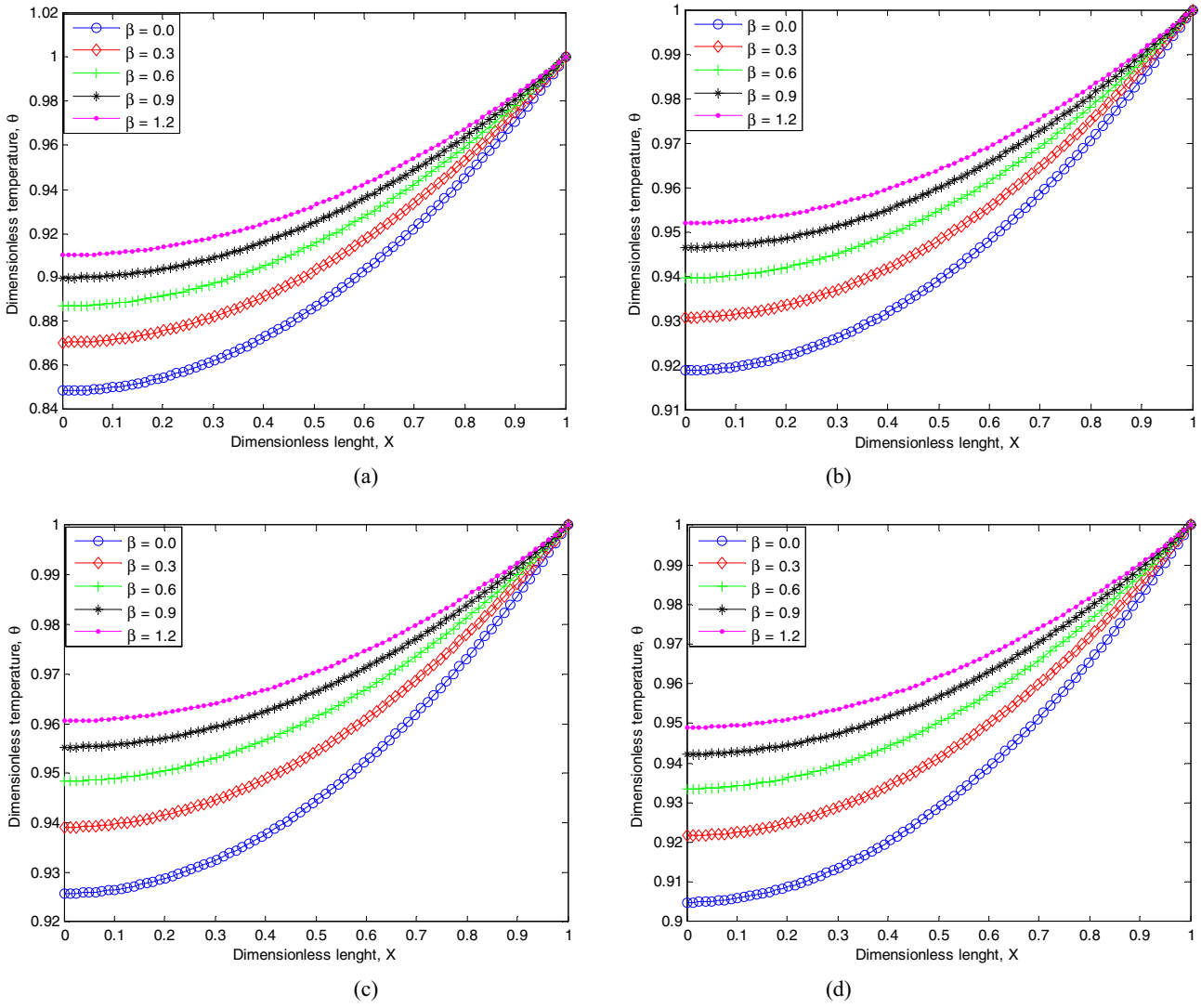

Fig. 2. Dimensionless temperature distribution in the fin parameters for varying thermo-geometric parameter when (a) S_h, = 1, Q = 0.4, γ = 0.2 (b)) S_h, = 1, Q = 0.6, γ = 0.2 (c) S_h, = 0.5, Q = 0.4, γ = 0.5 (d)) S_h, = 0.5, Q = 0.4, γ = 0.2.

In order to find exact analytical solution for Eq. (36), taking the transformation $\frac{d\theta}{dX} = \phi$, we arrived at

$$\phi\frac{d\phi}{dX} - S_h\theta^2 + S_hQ\gamma\theta + S_hQ = 0 \tag{37}$$

On integrating Eq. (37) wrt θ, we have

$$\frac{\phi^2}{2} - \frac{S_h}{3}\theta^3 + \left(\frac{S_hQ\gamma}{2}\right)\theta^2 + S_hQ\theta = C \tag{38}$$

Recall that $\phi = \frac{d\theta}{dX} \quad \rightarrow \phi^2 = \left(\frac{d\theta}{dX}\right)^2$

Therefore, Eq. (38) becomes

$$\frac{1}{2}\left(\frac{d\theta}{dX}\right)^2 - \frac{S_h}{3}\theta^3 + \left(\frac{S_hQ\gamma}{2}\right)\theta^2 + S_hQ\theta = C \tag{39}$$

With the application of the first boundary condition, $X = 1, \quad \frac{d\theta}{dX} = 0 \quad \rightarrow X = 1, \quad \theta = \theta_o$

$$C = -\frac{S_h}{3}\theta_o^3 + \left(\frac{S_hQ\gamma}{2}\right)\theta_o^2 + S_hQ\theta_o \tag{40}$$

On substituting Eq. (40) into Eq. (39), we arrived at

$$\frac{1}{2}\left(\frac{d\theta}{dX}\right)^2 - \frac{S_h}{3}(\theta^3 - \theta_o^3) + \left(\frac{S_hQ\gamma}{2}\right)(\theta^2 - \theta_o^2) + S_hQ(\theta - \theta_o) = 0 \tag{41}$$

Which could be written as

$$\left(\frac{d\theta}{dX}\right)^2 - \frac{2S_h}{3}\theta^3 + (S_hQ\gamma)\theta^2 + 2S_hQ\theta + \frac{2S_h}{3}\theta_o^3 - (S_hQ\gamma)\theta_o^2 - 2S_hQ\theta_o = 0 \tag{42}$$

Then

$$dX = \frac{-d\theta}{\sqrt{\frac{2S_h}{3}\theta^3 - (S_hQ\gamma)\theta^2 - 2S_hQ\theta - \frac{2S_h}{3}\theta_o^3 + (S_hQ\gamma)\theta_o^2 + 2S_hQ\theta_o}} \tag{43}$$

Since θ decreases as x increases, the negative sign is used in when taking the square root.

Integrating Eq. (44)

$$\int_0^X dX = -\int_{\theta_o}^{\theta} \frac{d\theta}{\sqrt{\frac{2S_h}{3}\theta^3 - S_hQ\gamma\theta^2 - 2S_hQ\theta - \frac{2S_h}{3}\theta_o^3 + S_hQ\gamma\theta_o^2 + 2S_hQ\theta_o}} \tag{44}$$

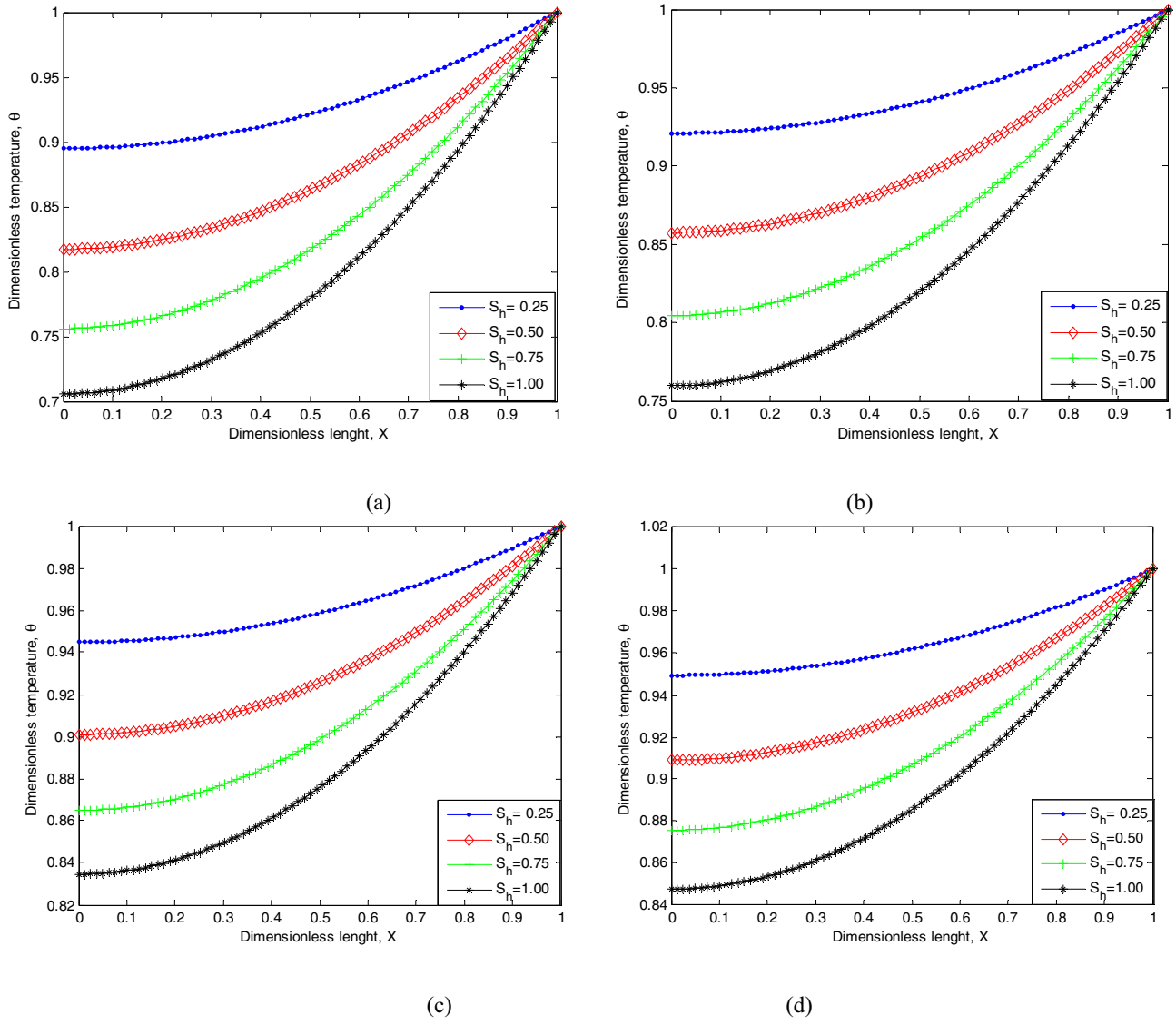

Fig. 3. Dimensionless temperature distribution in the fin parameters for varying thermo-geometric parameter when (a) $\beta = 0$, $Q = 0$, $\gamma = 0$ (b) $\beta, = 0.4$, $Q = 0$, $\gamma = 0$ (c) $\beta = 0.4$, $Q = 0.3$, $\gamma = 0$ (d) $\beta, = 0.4$, $Q = 0.3$, $\gamma = 0.2$.

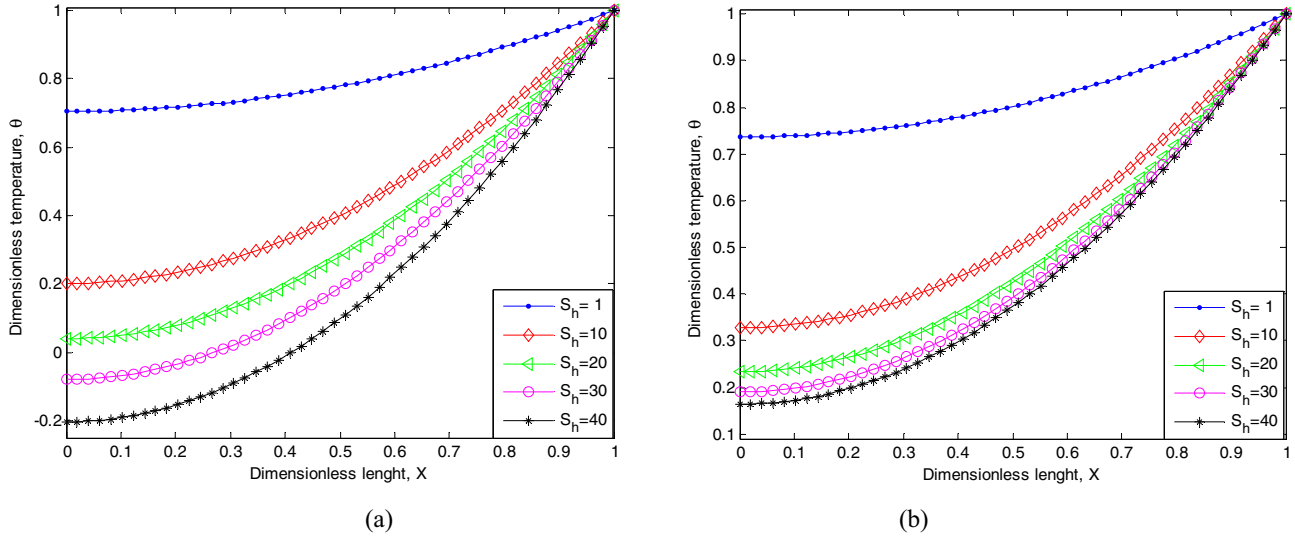

Fig. 4. Effects of porous parameter on the temperature distribution in the fin parameters when (a) $\beta = 0$, $Q = 0$, $\gamma = 0$, (b) $\beta, = 0.4$, $Q = 0.1$, $\gamma = 0$.

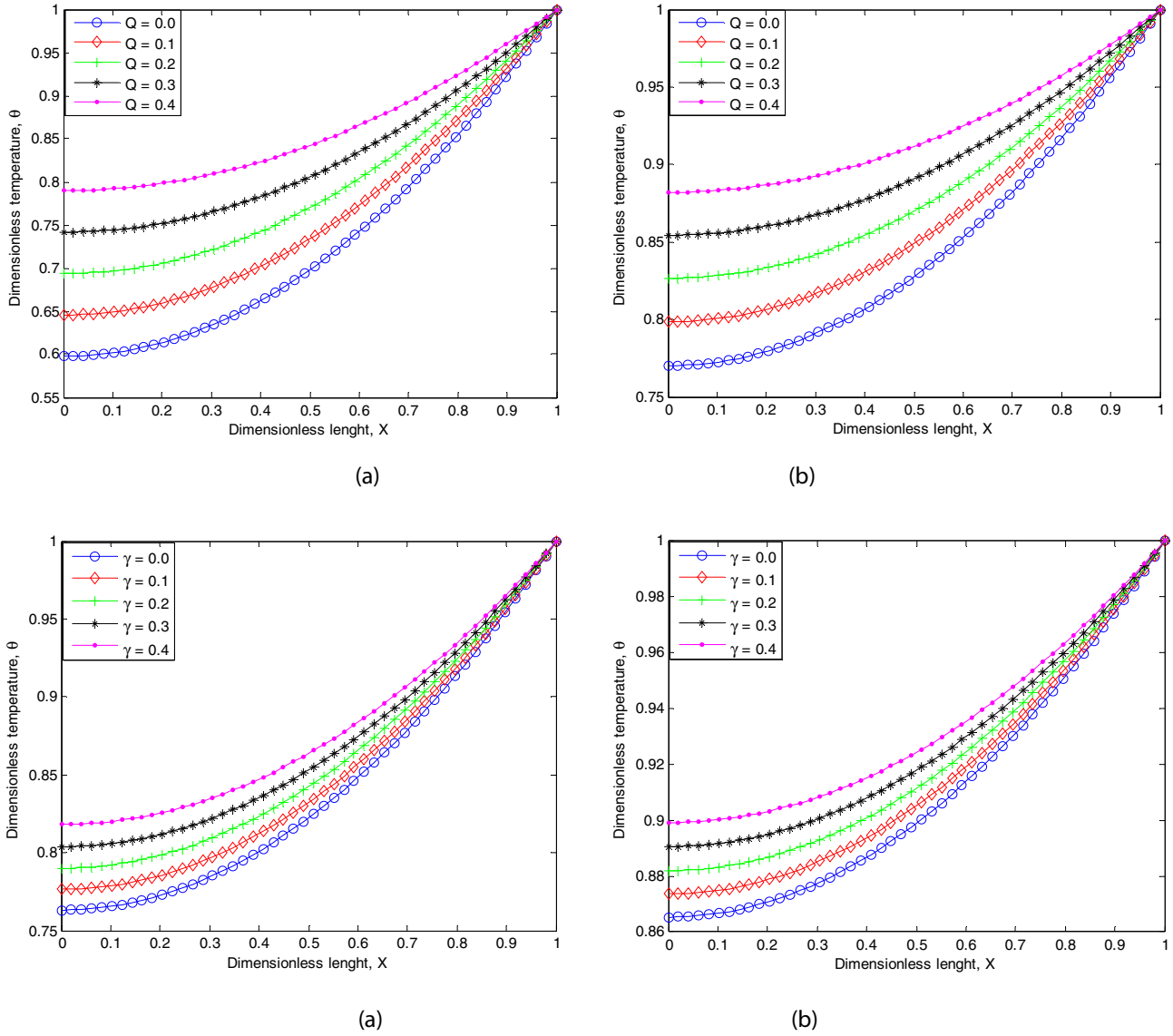

Fig. 5. Dimensionless temperature distribution in the fin parameters for varying thermo-geometric parameter when (a) $S_h = 1$, $\beta = -0.5$, $\gamma = 0.2$ (b) $S_h = 1$, $\beta, = 0.5$, $\gamma = 0.2$ (c) $S_h = 1$, $\beta = -0.5$, $Q = 0.4$ (d) $S_h = 1$, $\beta = 0.5$, $Q = 0.4$.

which gives

$$X = \int_{\theta}^{\theta_o} \frac{d\theta}{\sqrt{\frac{2S_h}{3}\theta^3 - S_h Q\gamma\theta^2 - 2S_h Q\theta - \frac{2S_h}{3}\theta_o^3 + S_h Q\gamma\theta_o^2 + 2S_h Q\theta_o}} \tag{45}$$

Suppose that

$$G(\theta; S_h, Q, \theta_o) = \int_{\theta}^{\theta_o} \frac{d\theta}{\sqrt{\frac{2S_h}{3}\theta^3 - S_h Q\gamma\theta^2 - 2S_h Q\theta - \frac{2S_h}{3}\theta_o^3 + S_h Q\gamma\theta_o^2 + 2S_h Q\theta_o}} \tag{46}$$

For instant [34]

where

$$\alpha_1 = \sqrt{57 - 12\theta_o - 12\theta_o^2}$$

$$\alpha_2 = \sqrt{6\theta^3 - 18\theta + 9\theta^2 - 6\theta_o^3 + 18\theta_o - 9\theta_o^2}$$

$$\alpha_3 = \sqrt{2 - 2\theta_o - 2\theta_o^2}$$

Therefore, the exact solution of Eq. (36) in implicit form is given by

$$X = G(\theta; S_h, Q, \theta_o) \tag{48}$$

$$G(\theta; 1, 1, \theta_o) = \sqrt{\frac{\alpha_1^2}{3 + 6\theta_o + \alpha_1}} \left\{ \frac{\left[\sqrt{\frac{3+6\theta_o+\alpha_1}{\alpha_1}} \sqrt{\frac{-3-6\theta_o+\alpha_1}{\alpha_1}} EllipticF\left(\sqrt{\frac{3+6\theta_o+\alpha_1}{2\alpha_1}}, \sqrt{\frac{2\alpha_1}{3+6\theta_o+\alpha_1}} \right) \alpha_2 - 3\sqrt{\frac{3+2\theta_o+\alpha_1+4\theta}{\alpha_1}} \sqrt{\theta_o - \theta} \sqrt{\frac{-3-2\theta_o+\alpha_1+4\theta}{\alpha_1}} EllipticF\left(\sqrt{\frac{3+2\theta_o+\alpha_1+4\theta}{2\alpha_1}}, \sqrt{\frac{2\alpha_1}{3+6\theta_o+\alpha_1}} \right) \alpha_3 \right]}{\alpha_2 \alpha_3} \right\} \tag{47}$$

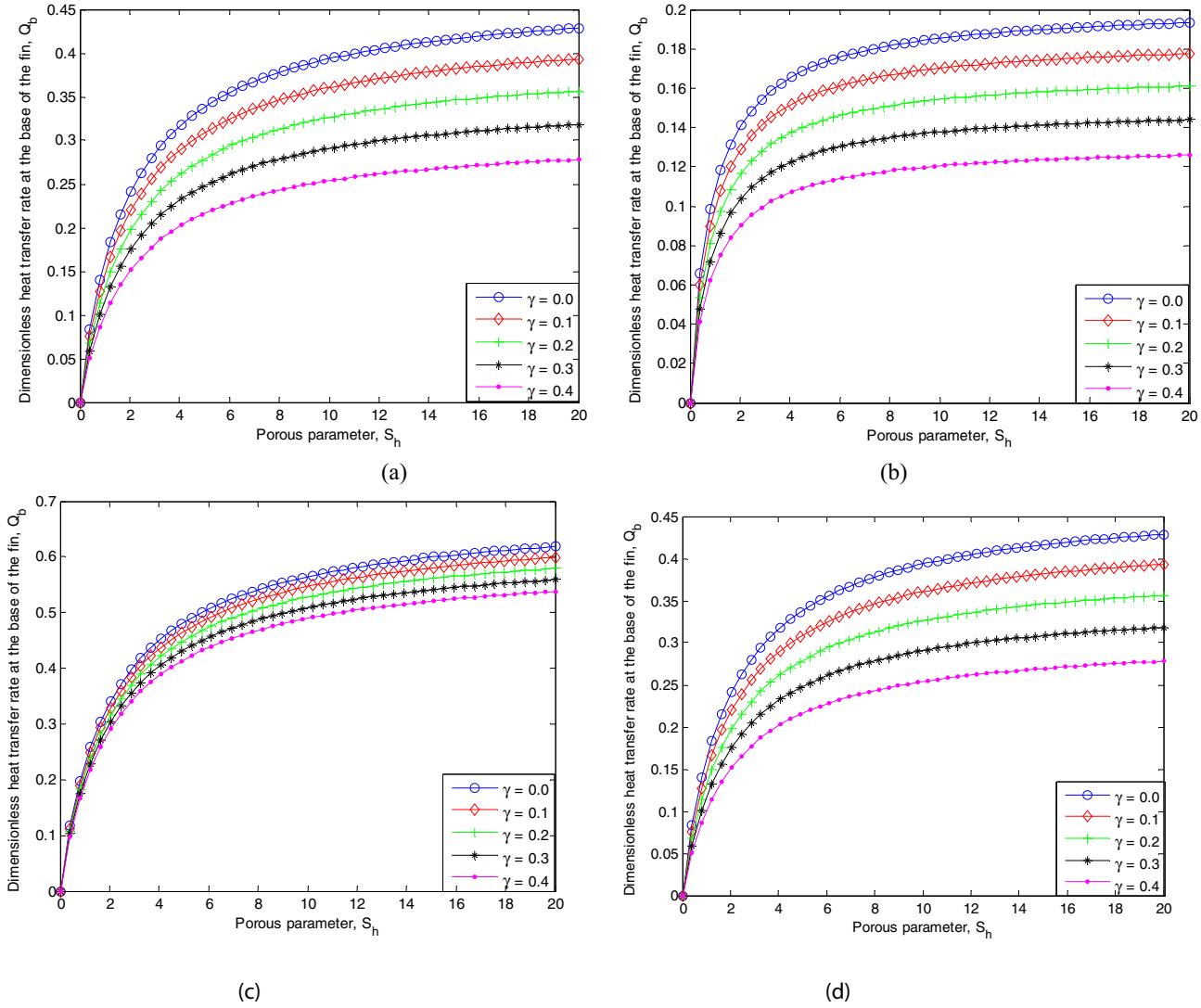

Fig. 6. Effects of temperature-dependent internal heat generation parameter on the dimensionless heat transfer rate in the fin when (a) β = −0.4, Q = 0.5 (b) β = 0.4, Q = 0.5 (c) β = −0.4, Q = 0.3 (d) β = 0.4, Q = 0.3.

Where the unknown θ_o in the solution can be determined from the second boundary condition

$$X = 0, \quad \theta = 1 \quad \rightarrow 1 = G(0; S_h, Q, \theta_o) \quad \rightarrow G(0; S_h, Q, \theta_o) = 1$$

i.e. for any given S_h, and Q, $\theta_o$is obtained from

$$G(0; S_h, Q, \theta_o) = 1 \tag{49}$$

And EllipticF in Eq. (47) is the incomplete elliptic integral of the first kind defined as

$$EllipticF(X, K) = \int_0^X \frac{d\tau}{\sqrt{1-\tau^2}\sqrt{1-K^2\tau^2}} \tag{50a}$$

This function can be exactly and analytically evaluated as follows

Let $\tau = sin\vartheta, \quad x = sin\phi$

$$EllipticF(\phi, K) = \int_0^\phi \frac{d\vartheta}{\sqrt{1-K^2 sin\vartheta}} \tag{50b}$$

In order to evaluate the integral, we expand the integral in the form

$$\frac{1}{\sqrt{1-K^2sin^2\vartheta}} = 1 + \frac{K^2}{2}sin^2\vartheta + \frac{3K^4}{8}sin^4\vartheta + \frac{5K^6}{16}sin^6\vartheta + \frac{35K^8}{128}sin^8\vartheta + \ldots \tag{51}$$

which could written as

$$\frac{1}{\sqrt{1-K^2sin^2\vartheta}} - 1 = \frac{K^2}{2}sin^2\vartheta + \frac{3K^4}{8}sin^4\vartheta + \frac{5K^6}{16}sin^6\vartheta + \frac{35K^8}{128}sin^8\vartheta + \ldots + \left(\Pi_{n=1}^{\infty}\frac{2n-1}{2n}\right)K^{2n}sin^{2n}\vartheta \tag{52}$$

Generally, we can write

$$\frac{1}{\sqrt{1-K^2sin^2\vartheta}} = 1 + \sum_{n=1}^{\infty}\left(\Pi_{n=1}^{\infty}\frac{2n-1}{2n}\right)K^{2n}sin^{2n}\vartheta \tag{53}$$

The above series is uniformly convergent for all ϑ, and may, therefore, be integrated term by term. Then, we have

$$EllipticF(\phi, K) = \int_0^\phi \left\{1 + \sum_{n=1}^{\infty}\left(\Pi_{n=1}^{\infty}\frac{2n-1}{2n}\right)K^{2n}sin^{2n}\vartheta\right\}d\vartheta \tag{54}$$

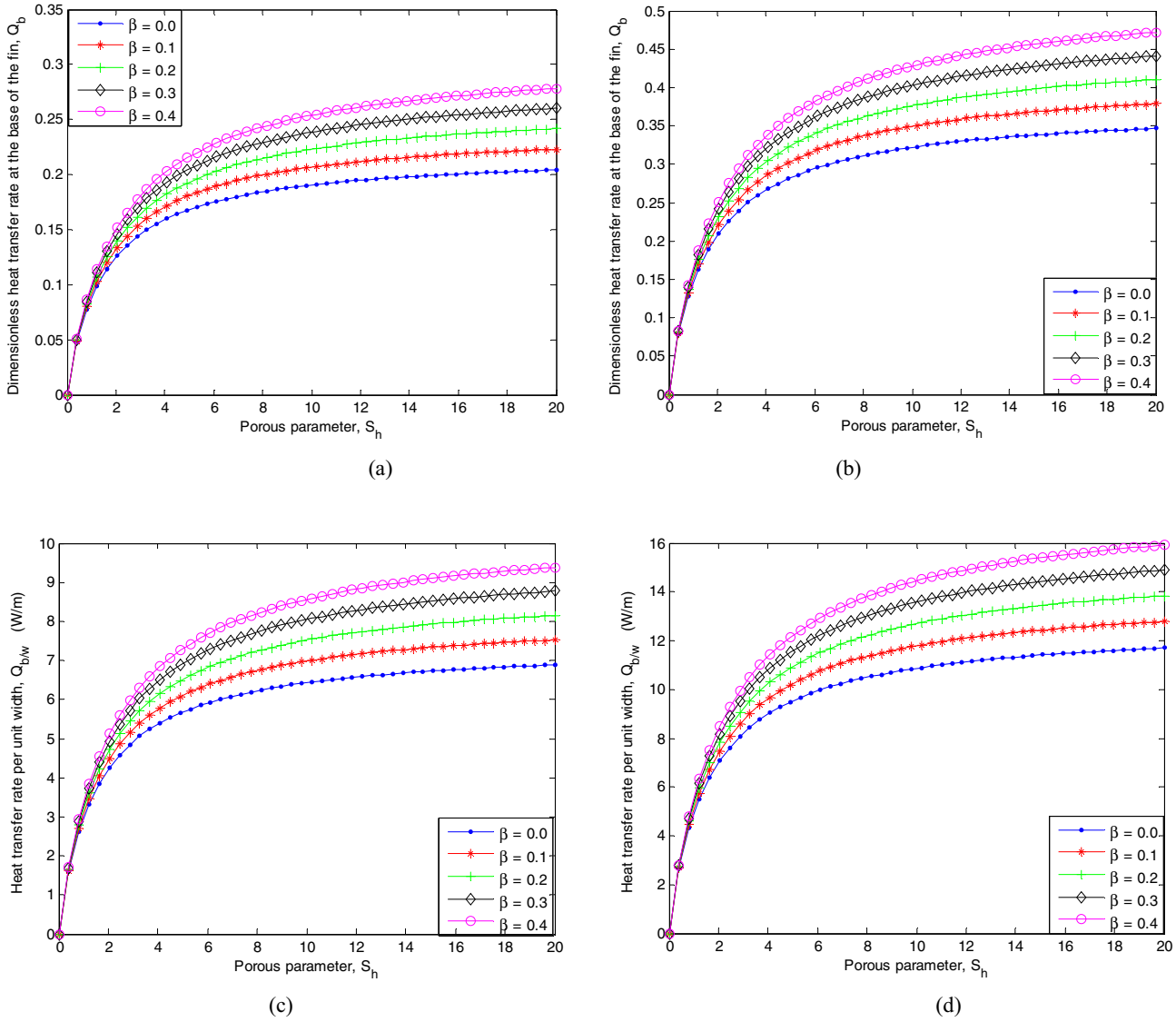

Fig. 7. Effects of temperature-dependent thermal conductivity parameter and fin thickness-length ratio on the dimensionless heat transfer rate at the base of the fin when (a) $\gamma = -0.4$, Q = 0.5 (b) $\gamma = 0.7$, Q = 0.3 (a) $t/L = 1/1000$, k = 45 W/mK; Tb = 373 K; Ta = 298 K; $\gamma = 0.4$, Q = 0.5 (b)$t/L = 1/1000$, k = 45 W/mK; Tb = 373 K; Ta = 298 K; $\gamma = -0.4$, Q = 0.5 $\gamma = 0.7$, Q = 0.3.

But

$$\int sin^{2n}\vartheta d\vartheta = \frac{-cos\vartheta}{2n}\left\{sin^{2n-1}\vartheta + \sum_{k=1}^{n-1}\frac{(2n-1)(2n-3)...(2n-2k+1)}{2^k(n-1)(n-2)...(n-k)}sin^{2n-2k-1}\vartheta\right\} + \frac{(2n-1)!!}{2^n n!}\vartheta \quad (55)$$

Therefore

$$EllipticF(\phi,K) = \left\{\phi + \sum_{n=1}^{\infty}\left(\Pi_{n=1}^{\infty}\frac{2n-1}{2n}\right)K^{2n} \times \left\{\begin{array}{l}\frac{-cos\phi}{2n}\left\{sin^{2n-1}\phi + \sum_{k=1}^{n-1}\frac{(2n-1)(2n-3)...(2n-2k+1)}{2^k(n-1)(n-2)...(n-k)}sin^{2n-2k-1}\phi\right\} \\ + \frac{(2n-1)!!}{2^n n!}\phi\end{array}\right\}\right\} \quad (56)$$

The symbolic and numerical calculations involved in the function $G(\theta; S_h, Q, \theta_o)$ were carried out via Wolfram's Mathematica.

4. Results and discussion

Effects of nonlinear thermal conductivity parameters on the dimensionless temperature distribution and by extension on the rate of heat transfer are shown in Fig. 2a–d. From the figures, it is shown that as the non-linear thermal conductivity parameter increases, the dimensionless temperature distribution in the fin decreases.

Figs. 3a–d show the effects of porous parameter or porosity on the temperature distribution in the porous fin. From the figures, as the porosity parameter increases, the temperature decreases rapidly and the rate of heat transfer through the fin increases as the temperature in the fin drops faster (becomes steeper reflecting high base heat flow rates) as depicted in the figures. The rapid decrease in fin temperature due to increase in the porosity parameter is because as porosity parameter, S_h increases and in consequent, the Darcy and Raleigh number increase, the permeability of the porous fin increases and therefore the ability of the working fluid to penetrate through the fin pores increases, the effect of buoyancy force increases and thus the fin transfers more heat

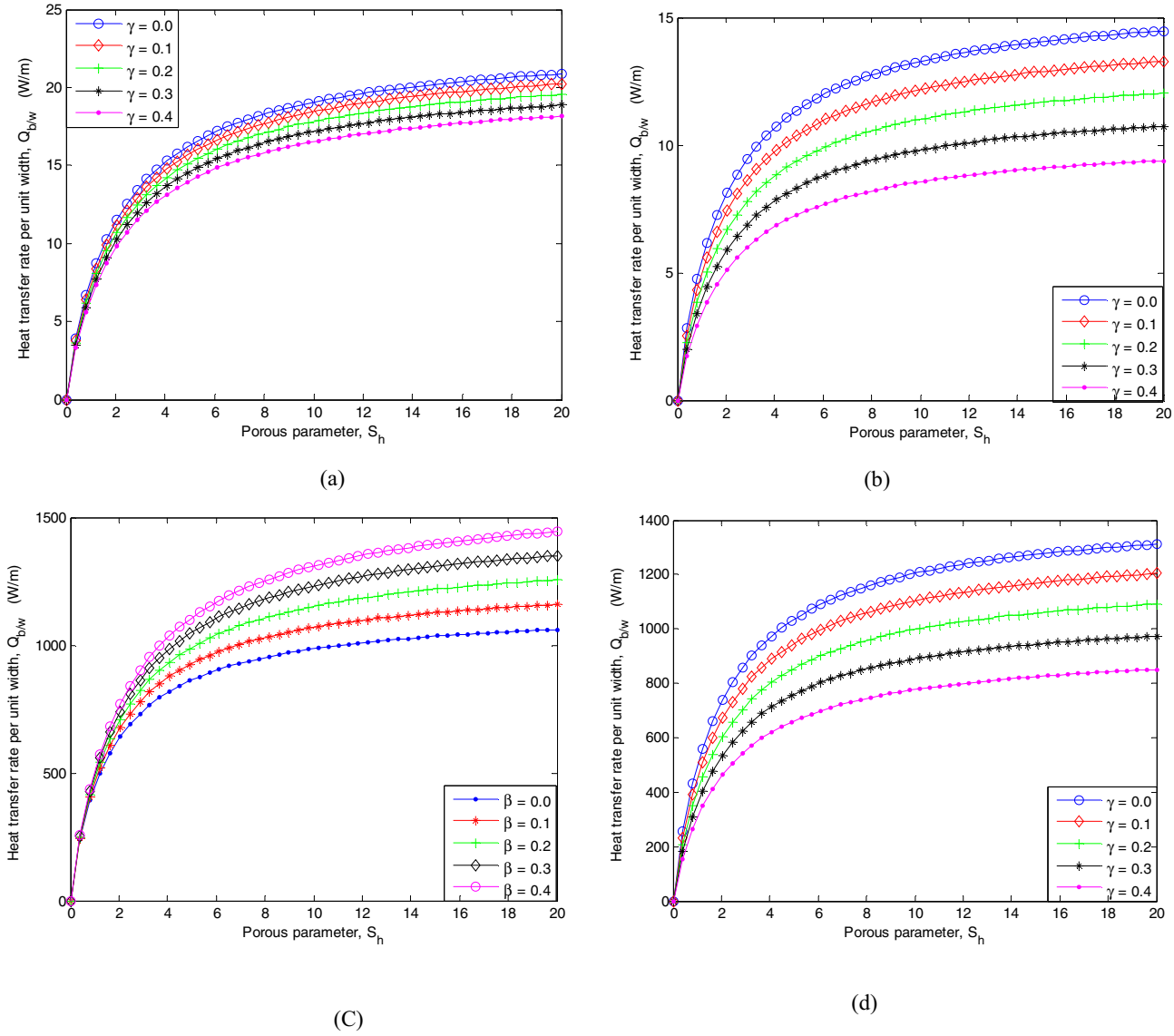

Fig. 8. Effects of temperature-dependent internal heat generation and fin thickness-length ratio on the dimensionless heat transfer rate in the fin when (a) t/L = 1/100; k = 45 W/Mk; T_b = 373 K; T_a = 298 K; β = 0.4, Q = 0.3 (b) t/L = 1/100, k = 45 W/Mk; T_b = 373 K; T_a = 298 K; γ = -0.4, Q = 0.5 β = 0.5, Q = 0.5 (c) t/L = 0.0102/0.125, k = 204 W/Mk; T_b = 373 K; T_a = 298 K; β = 0.7, Q = 0.3 (d) t/L = 0.0102/0.125, k = 204 W/Mk; T_b = 373 K; T_a = 298 K; Q = 0.5 β = 0.4, Q = 0.5.

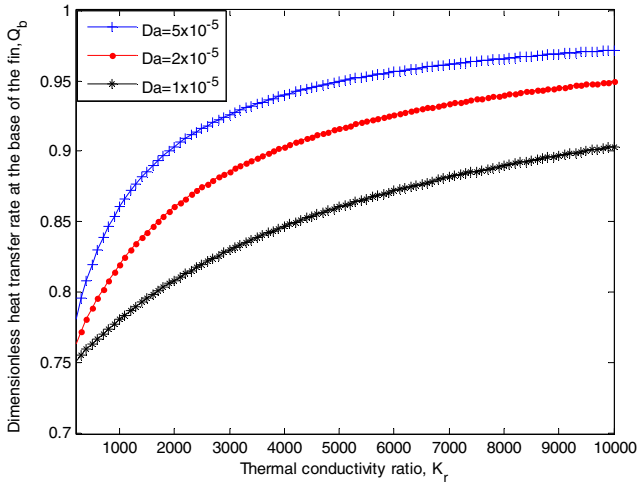

Fig. 9. Effects of Darcy number on dimensionless heat transfer rate.

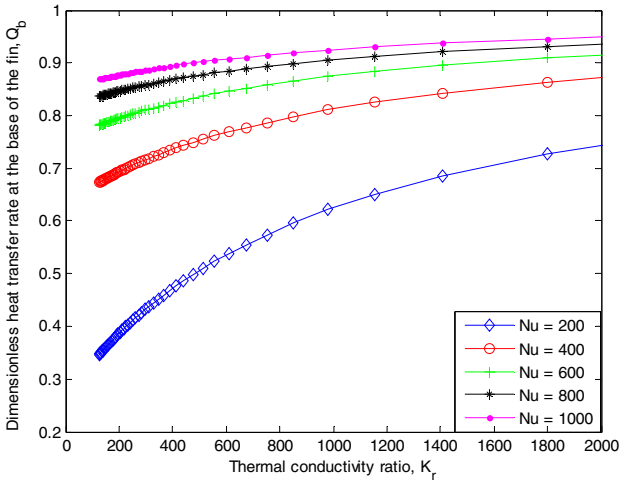

Fig. 10. Effects of Nusselt number on dimensionless heat transfer rate.

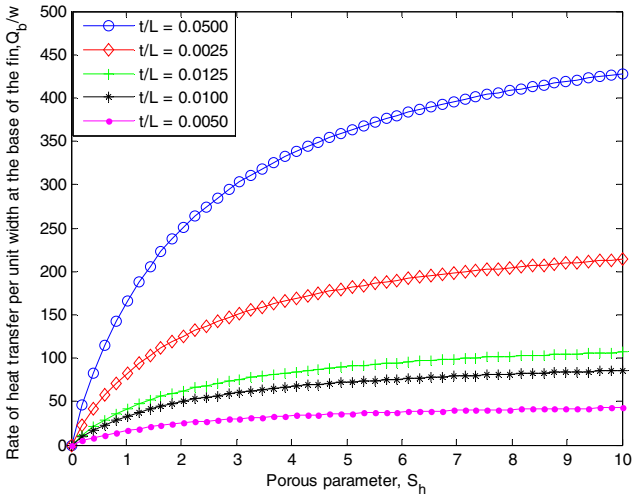

Fig. 11. Effects of length-thickness ratio on dimensionless heat transfer rate.

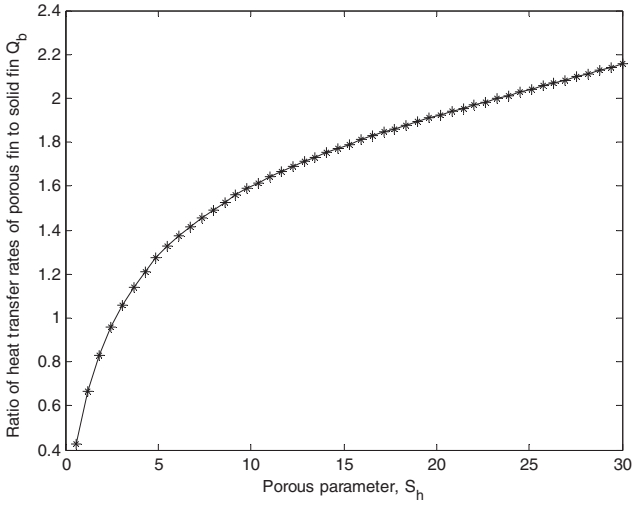

Fig. 12. Ratio of the porous fin to solid fin heat transfer rate with S_h.

and the rate of heat transfer from the fin is enhanced and the thermal performance of the fin is increased. It could therefore be stated that increase in the porosity of the fin improves fin efficiency due to increasing in convection heat transfer.

The effects of the porosity and the internal heat generation on the thermal stability of the fin is shown in Fig. 4a and b, it is obvious that as porous parameter, S_h increases to a certain value, the dimensionless temperature distribution at the fin tip results in negative value (which shows thermal instability) at $x = 0$, contradicting the assumption made in the analysis. This fact was not established in the Kiwan [3] numerical analysis of the same problem for the large values of S_h. From the analysis of the present work, the limiting value of S_h for thermal instability for constant thermal properties without internal heat generation is approximately $4\sqrt{34}$. However, the value of porosity parameter for the thermal stability increases with increase in internal heat generation parameter, Q (Fig. 4b) and thermal conductivity parameters, β.

Figs. 5a–d depict the effects of temperature-dependent internal heat generation parameter on the temperature distribution in the porous fin while Figs. 6a–d show the effects of temperature-dependent internal heat generation on the rate of heat transfer i.e. fin thermal performance at different porous parameters. From the figures, as the temperature-dependent internal heat generation parameter increases, the temperature gradient and consequently, the rate of heat transfer in the fin decreases. Also, the figures show that the rate of heat transfer at the base of the fin increases as the porous parameter or porosity increases.

Actually, a major important analysis in the fin problem is the determination of the rate of heat transfer at the base of the fin. Figs. 7a-d show the effects of temperature-dependent thermal conductivity parameter and fin thickness-length ratio, t/L, on the dimensionless heat transfer rate at the base of the fin while Fig. 8a-deffects of temperature-dependent internal heat generation parameter and fin thickness-length ratio on the dimensionless heat transfer rate at the base of the fin at different porous parameters. From the figures, it could be deducted that the temperature-dependent thermal conductivity parameter, porosity and fin thickness ratio have direct and significant effects on the rate of heat transfer at the base of the fin. Increase in the dimensionless thickness parameter (fin thickness-length ratio) results in increase in the rate of heat transfer at the base of the fin.

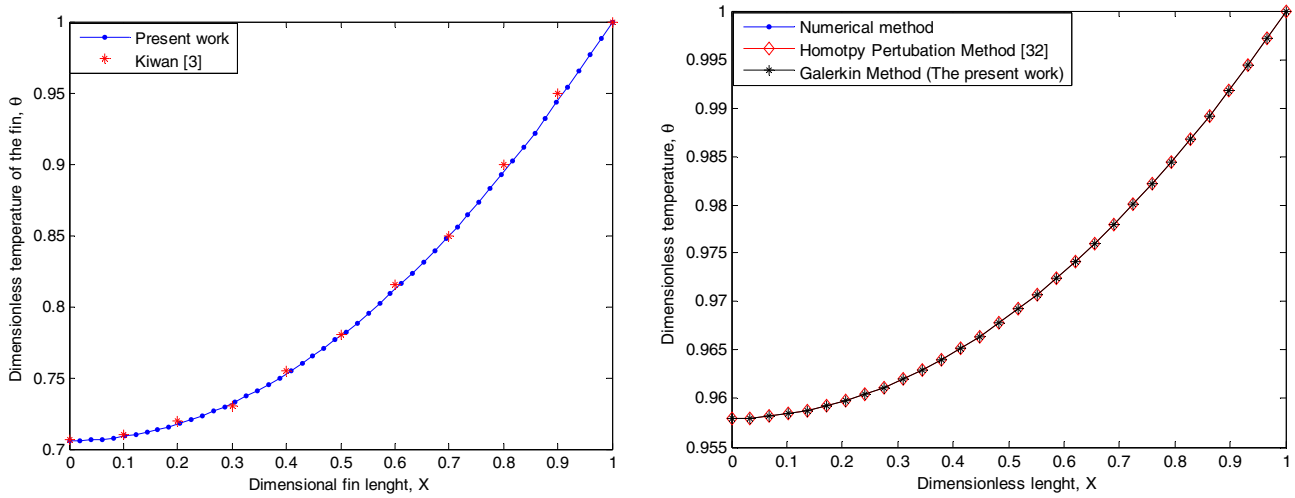

(a) (b)

Fig. 13. Comparison of results for $S_h = 1$.

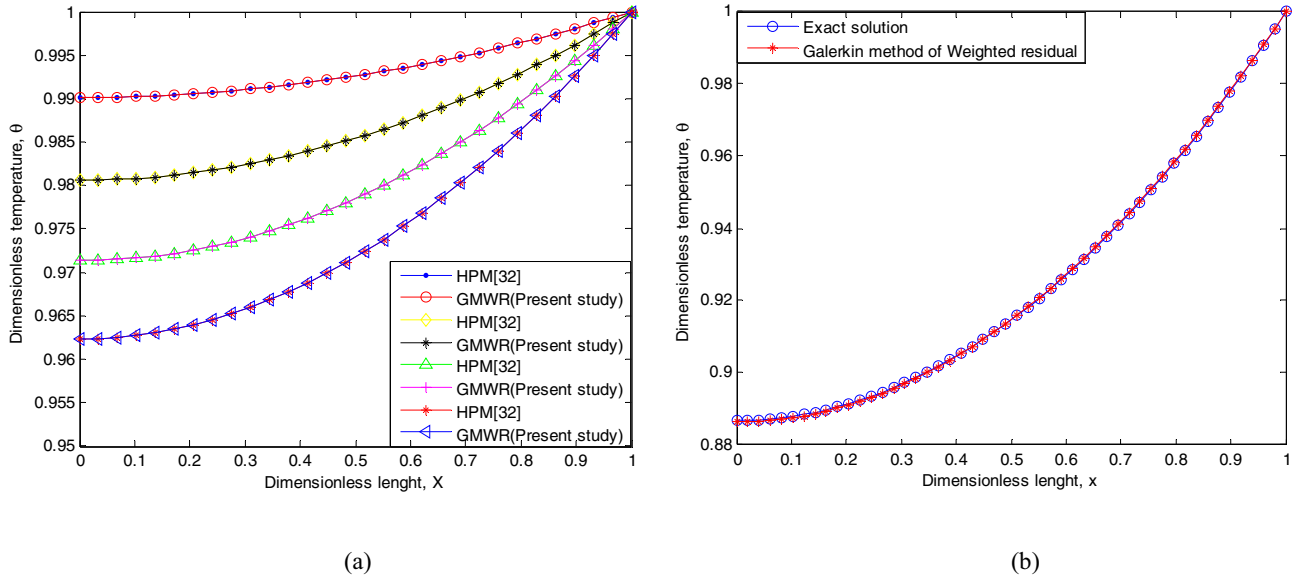

Fig. 14. (a) Comparison of GMWR and HPM results at different porosity numbers (b) Comparison of GMWR and Exact result.

Table 1
Table of comparison of results.

X	NM	HPM [55]	GWRM (The Present study)	Absolute Error in HPM	Absolute Error in GWRM
0.0	0.9581	0.9581	0.9581	0.0000	0.0000
0.1	0.9585	0.9585	0.9585	0.0000	0.0000
0.2	0.9597	0.9597	0.9597	0.0000	0.0000
0.3	0.9618	0.9618	0.9618	0.0000	0.0000
0.4	0.9647	0.9647	0.9647	0.0000	0.0000
0.5	0.9685	0.9685	0.9685	0.0000	0.0000
0.6	0.9730	0.9730	0.9730	0.0000	0.0000
0.7	0.9785	0.9785	0.9785	0.0000	0.0000
0.8	0.9846	0.9846	0.9848	0.0000	0.0000
0.9	0.9919	0.9919	0.9919	0.0000	0.0000
1.0	1.0000	1.0000	1.0000	0.0000	0.0000

The study of the effects of some dimensionless numbers that evolved during the analysis of the porous fin on the thermal performance of the fin is very essential. In other to carry out such study, some values were used. For the sake of comparison, these values are the same with the values used in the study of porous fin by Kiwan and Al-Nimr [1]. Fig. 9 shows the effects of Darcy number on the dimensionless rate of heat transfer. Increasing Darcy number, Da causes an increase in the heat transfer rate from the fin. This is because when the Darcy number and consequently permeability reduces, collision among the fluid flow and the pores of the porous is increased. Thus the passing fluids gave more space to contact with the porous media which has internal heat generation. Consequently, the fin temperature is increased by decreasing the Da number.

Effects of Nusselt number on the rate of heat transfer at the base of the fin is depicted in Fig. 10. It shows that as Nu increases more heat are drawn from the fin base. However, at high values of the porosity parameter S_h, increasing Nu has no significant influence on the heat transfer from the base of the fin. This is because as the porosity parameter S_h increases the temperature at the fin tip reaches the ambient temperature of the surrounding fluid and thus the driving force for heat transfer from the fin tip reduces. This leads to a significant reduction from the use of high values of Nu at the tip [3]. Increasing *t/L*or decreasing thermal conductivity parameter, K_r increases S_h and thus increasing the rate of heat transfer at the base of the fin. Moreover, increasing L or decreasing K_r tends to reduce the heat transfer rate from the fin. From the result, for the different values of fin thicknesses, the respective optimum values (values beyond which a further increase on S_h or L has no significant change on the heat transfer rate) for S_h and L can be established (Fig. 11). Also, ncrease in fin thickness-length ratio, *t/L*, increases the rate of heat transfer from the base of the fin as shown in Fig. 11. However, as fin thickness-length ratio increases up to some certain values for the different fin thickness-length *ratio* considered, optimum points are reached where further increase in *t/L* has no significant influence on the heat transfer rate from the base of the fin. As the fin length increases, the temperature of the part far from the fin base approaches the working fluid temperature. This implies that the driving force for natural convection decreases and leads (in porous fins) to less fluid infiltrated through the pores of the porous domain. Also, this implies that no significant improvements is attained if the fin length is further increased. This scenario is not only peculiar to porous fin, it also occurs in solid fin.

In order to make a comparison between the heat transfer rates from a porous fin with that from a solid fin, the ratio of the heat transfer rate between the porous fin and solid are established as given by Eq. (34). Fig. 12 shows the effects of porosity number on the ratio of heat transfer rate between the porous fin and solid. Increase in porosity number, S_h, implies increase in Darcy and Rayleigh numbers. While the increase in Darcy number, *Da* increases the permeability of the fin. Increase in *Ra* number leads to more effects of buoyancy force and consequently heat transfer rate due to convection mechanism. Therefore, high values of S_h or *Da* and

Ra lead high value of the ratio of heat transfer rate between the porous fin and solid and enhanced heat transfer between the fin and the air flow.

The results of the approximate analytical method used in this work was verified with the results of the fourth-Order Runge-Kutta with shooting algorithm as presented by Kiwan [3], and also with the numerical method (NM) using bvp4c in MATLAB and the results of homotopy perturbation method (HPM) as presented by Petroudi et al. [32] as shown in Figs. 13 and 14a and with the exact analytical solution results as shown in Fig. 14b. It is depicted that the Galerkin's method is highly accurate and shows excellent agreement with the results of the NM and the HPM. It was established that when $S_h > 1$, the HPM solutions for $\beta = \pm 0.4$ are very weak and provide unreasonable results. HPM solution fails when porosity parameter increases to a large number. This shortcoming in the solution method is not only peculiar to HPM, it is also experienced when using ADM [33] coupled with the additional task tasks of finding Adomian polynomials. The results show that the GMWR is very effective and it is a convenient tool to solve the nonlinear fin problems under different conditions.

Table 1 shows comparison of results and the errors in the method used in this study. It could be inferred from the table that the Galerkin's method is highly accurate and agrees very well with the results of numerical and homotopy perturbation methods.

5. Conclusion

In this work, thermal performance analysis in a natural convection porous fin temperature-dependent thermal properties and internal heat generation has been analyzed using Galerkin's method of weighted residual. The developed symbolic heat transfer models were used to investigate the effects of various parameters on the thermal performance of the porous fin. Increasing the porosity, Nusselt, Darcy and Rayleigh numbers and thickness-length ratio of the fin increase the rate of heat transfer from the base of the fin and consequently improve the efficiency of the fin. Also, decreasing thermal conductivity parameter, K_r results in increase in the rate of heat transfer from the base of the fin. However, an optimum value is reached beyond which further increase in porosity, Nusselt, Darcy and Rayleigh numbers, thermal conductivity ratio and thickness-length ratio has no significant influence on the rate of heat transfer. The results of the Galerkin's method used in the work was verified with the numerical method using Runge-Kutta method. The Galerkin's method results for the second-order approximation function used are in excellent agreement with results of the numerical method and that of homotopy perturbation method as found in literature.

References

[1] S. Kiwan, A. Al-Nimr, Using porous fins for heat transfer enhancement, ASME J. Heat Transfer 123 (2001) 790–795.
[2] S. Kiwan, Effect of radiative losses on the heat transfer from porous fins, Int. J. Therm. Sci. 46 (2007) 1046–1055.
[3] S. Kiwan, Thermal analysis of natural convection porous fins, Tran. Porous Media 67 (2007) 17–29.
[4] S. Kiwan, O. Zeitoun, Natural convection in a horizontal cylindrical annulus using porous fins, Int. J. Numer. Heat Fluid Flow 18 (5) (2008) 618–634.
[5] R.S. Gorla, A.Y. Bakier, Thermal analysis of natural convection and radiation in porous fins, Int. Commun. Heat Mass Transfer 38 (2011) 638–645.
[6] B. Kundu, D. Bhanji, An analytical prediction for performance and optimum design analysis of porous fins, Int. J. Refrig. 34 (2011) 337–352.
[7] B. Kundu, D. Bhanja, K.S. Lee, A model on the basis of analytics for computing maximum heat transfer in porous fins, Int. J. Heat Mass Transfer 55 (25–26) (2012) 7611–7622.
[8] A. Taklifi, C. Aghanajafi, H. Akrami, The effect of MHD on a porous fin attached to a vertical isothermal surface, Transp. Porous Med. 85 (2010) 215–231.
[9] D. Bhanja, B. Kundu, Thermal analysis of a constructal T-shaped porous fin with radiation effects, Int. J. Refrig. 34 (2011) 1483–1496.
[10] B. Kundu, Performance and optimization analysis of SRC profile fins subject to simultaneous heat and mass transfer, Int. J. Heat Mass Transfer 50 (2007) 1545–1558.
[11] S. Saedodin, S. Sadeghi, Temperature distribution in long porous fins in natural convection condition, Middle-East J. Sci. Res. 13 (6) (2013) 812–817.
[12] S. Saedodin, M. Olank, Temperature distribution in porous fins in natural convection condition, J. Am. Sci. 7 (6) (2011) 476–481.
[13] M.T. Darvishi, R.S.R. Gorla, R.S. Khani, F. Khani, A.E. Aziz, Thermal performance of a porus radial fin with natural convection and radiative heat losses, Therm. Sci. 19 (2) (2015) 669–678.
[14] M. Hatami, D.D. Ganji, Thermal performance of circular convective-radiative porous fins with different section shapes and materials, Energy Convers. Manage. 76 (2013) 185–193.
[15] M. Hatami, D.D. Ganji, Thermal behavior of longitudinal convective–radiative porous fins with different section shapes and ceramic materials (SiC and Si3N4), Int. J. Ceram. Int. 40 (2014) 6765–6775.
[16] M. Hatami, A. Hasanpour, D.D. Ganji, Heat transfer study through porous fins (Si3N4 and AL) with temperature-dependent heat generation, Energy Convers. Manage. 74 (2013) 9–16.
[17] M. Hatami, D.D. Ganji, Investigation of refrigeration efficiency for fully wet circular porous fins with variable sections by combined heat and mass transfer analysis, Int. J. Refrig. 40 (2014) 140–151.
[18] M. Hatami, G.H.R.M. Ahangar, D.D. Ganji, K. Boubaker, Refrigeration efficiency analysis for fully wet semi-spherical porous fins, Energy Convers. Manage. 84 (2014) 533–540.
[19] R.S.R. Gorla, M.T. Darvishi, F. Khani, Effects of variable Thermal conductivity on natural convection and radiation in porous fins, Int. Commun. Heat Mass Transfer 38 (2013) 638–645.
[20] A. Moradi, T. Hayat, A. Alsaedi, Convective-radiative thermal analysis of triangular fins with temperature-dependent thermal conductivity by DTM, Energy Convers. Manage. 77 (2014) 70–77.
[21] S. Saedodin, M. Shahbabaei, Thermal analysis of natural convection in porous fins with homotopy perturbation method (HPM), Arab. J. Sci. Eng. 38 (2013) 2227–2231.
[22] H. Ha, D.D. Ganji, M. Abbasi, Determination of temperature distribution for porous fin with temperature-dependent heat generation by homotopy analysis method, J. Appl. Mech. Eng. 4 (1) (2005).
[23] H.A. Hoshyar, I. Rahimipetroudi, D.D. Ganji, A.R. Majidian, Thermal performance of porous fins with temperature-dependent heat generation via Homotopy perturbation method and collocation method, J. Appl. Math. Computat. Mech. 14 (4) (2015) 53–65.
[24] Y. Rostamiyan, D.D. Ganji, I.R. Petroudi, M.K. Nejad, Analytical investigation of nonlinear model arising in heat transfer through the porous fin, Therm. Sci. 18 (2) (2014) 409–417.
[25] S.E. Ghasemi, P. Valipour, M. Hatami, D.D. Ganji, Heat transfer study on solid and porous convective fins with temperature-dependent heat – generation using efficient analytical method, J. Cent. South Univ. 21 (2014) 4592–4598.
[26] A. Azizand, M.N. Bouaziz, A least squares method for a longitudinal fin with temperature dependent internal heat generation and thermal conductivity, Energy Convers Manage. 52 (2011) 2876–2882.
[27] A. Fernandez, On some approximate methods for nonlinear models, Appl. Math. Comput. 215 (2009) 168–174.
[28] R.W. Lewis, P. Nithiarasu, K.N. Seetharamu, Fundamental of the Finite Element Method for Heat and Fluid Flow, John Wiley and Sons, 2004.
[29] M.G. Sobamowo, Thermal analysis of longitudinal fin with temperature-dependent properties and internal heat generation using Galerkin's method of weighted residual, Appl. Therm. Eng. 99 (2016) 1316–1330.
[30] D.D. Ganji, M. Rahgoshay, M. Rahimi, M. Jafari, Numerical investigation of fin efficiency and temperature distribution of conductive, convective and radiative straight fins, Int. J. Res. Rev. Appl. Sci. 4 (3) (2010) 230–237 (1).
[31] C.W. Bert, Improved approximate methods for analysis steady heat conduction, Commun. Appl. Numer. Methods 2 (1986) 587–592.
[32] I.R. Petroudi, D.D. Ganji, A.B. Shotorban, M.K. Nejad, E. Rahimi, R. Rohollahtabar, F. Taherinia, Semi-analytical method for solving nonlinear equation arising in natural convection porous fin, Therm. Sci. 16 (5) (2012) 1303–1308.
[33] F. Khani, M. Ahmadzadeh Raji, H. Hamedi Nejad, Analytical solutions and efficiency of the nonlinear fin problem with temperature-dependent thermal conductivity and heat transfer coefficient, Commun. Nonlinear Sci. Numer. Simul. 14 (2009) 3327–3338.
[34] S. Abbasbandy, E. Shivanianand, I. Hashim, Exact analytical solution of a forced convection in porous-saturated duct, Commun. Nonlinear Sci. Numer. Simul. 16 (2011) 3981–3989.